Deficiency of the *ywhaz* gene, involved in neurodevelopmental disorders, alters brain activity and behaviour in zebrafish

Ester Antón-Galindo[1,2,3,4]*, Elisa Dalla Vecchia[5]*, Javier G Orlandi[6], Gustavo Castro[7], Emilio J Gualda[7], Andrew MJ Young[8], Marc Guasch-Piqueras[1,3], Concepció Arenas[1], Carlos Herrera-Úbeda[1,3], Jordi García-Fernàndez[1,3], Fernando Aguado[9,10], Pablo Loza-Alvarez[7], Bru Cormand[1,2,3,4#], William HJ Norton[5#], Noèlia Fernàndez-Castillo[1,2,3,4#]

[1]Departament de Genètica, Microbiologia i Estadística, Facultat de Biologia, Universitat de Barcelona, Barcelona, Catalunya, 08028, Spain

[2]Centro de Investigación Biomédica en Red de Enfermedades raras (CIBERER), Spain

[3]Institut de Biomedicina de la Universitat de Barcelona (IBUB), Barcelona, Catalunya, 08028, Spain

[4]Institut de recerca Sant Joan de Déu (IRSJD), Espluges de Llobregat, Catalunya, 08950, Spain

[5]Department of Genetics and Genome Biology, College of Life Sciences, University of Leicester, Leicester, LE1 7RH, United Kingdom

[6]RIKEN Center for Brain Science, Wako-shi, Saitama 351-0198, Japan

[7]ICFO - Institut de Ciencies Fotoniques, The Barcelona Institute of Science and Technology, Castelldefels, Catalunya, 08860, Spain

[8]Department of Neuroscience, Psychology and Behaviour, College of Life Sciences, University of Leicester, Leicester, LE1 7RH, United Kingdom

[9]Departament de Biologia cel·lular, Fisiologia i Immunologia, Facultat de Biologia, Universitat de Barcelona, Barcelona, Catalunya, 08028, Spain

[10]Institute of Neurosciences, Universitat de Barcelona, Barcelona, Catalunya, 08028, Spain

* equally contributed to this work; [#] equally supervised this work

Corresponding authors:

Noèlia Fenàndez-Castillo, noefernandez@ub.edu, Departament de Genètica, Microbiologia i Estadística, Facultat de Biologia, Universitat de Barcelona, Barcelona, Catalunya, 08028, Spain, Tel: +34 934037082.

William HJ Norton, whjn1@leicester.ac.uk, Department of Genetics and Genome Biology, College of Life Sciences, University of Leicester, Leicester, LE1 7RH, United Kingdom, Tel: 0116 252 5078.

Bru Cormand, bcormand@ub.edu, Departament de Genètica, Microbiologia i Estadística, Facultat de Biologia, Universitat de Barcelona, Barcelona, Catalunya, 08028, Spain, Tel: +34 934021013.

ABSTRACT

Genetic variants in *YWHAZ* contribute to psychiatric disorders such as autism spectrum disorder and schizophrenia, and have been related to an impaired neurodevelopment in humans and mice. Here, we have used zebrafish to investigate the mechanisms by which *YWHAZ* contributes to neurodevelopmental disorders. We observed that *ywhaz* expression was pan-neuronal during developmental stages and restricted to Purkinje cells in the adult cerebellum, cells that are described to be reduced in number and size in autistic patients. We then performed whole-brain imaging in wild-type and *ywhaz* CRISPR/Cas9 knockout (KO) larvae and found altered neuronal activity and connectivity in the hindbrain. Adult *ywhaz* KO fish display decreased levels of monoamines in the hindbrain and freeze when exposed to novel stimuli, a phenotype that can be reversed with drugs that target monoamine neurotransmission. These findings suggest an important role for *ywhaz* in establishing neuronal connectivity during development and modulating both neurotransmission and behaviour in adults.

INTRODUCTION

The *YWHAZ* gene has been related to several psychiatric disorders in different human studies. Genetic studies have associated *YWHAZ* polymorphisms with major depression and schizophrenia [1, 2]. A protein-protein interaction analysis including all genes found mutated in an exome sequencing study of autism spectrum disorder (ASD) in multiplex families reported YWHAZ as the main node of the network [3], and a heterozygous frameshift mutation in the *YWHAZ* gene, transmitted from a mother with depression to her two siblings diagnosed with autism spectrum disorder (ASD) and attention deficit/hyperactivity disorder (ADHD), was found to have functional implications [2]. Furthermore, decreased expression of the *YWHAZ* gene and low levels of the corresponding 14-3-3ζ protein were reported in *postmortem* brains of patients with neurodevelopmental disorders like ASD and schizophrenia [2, 4, 5], and 14-3-3 protein levels are reduced in platelets and pineal glands of ASD patients [6, 7]. However, even though evidence points to a contribution of *YWHAZ* to neurodevelopmental and psychiatric disorders, the mechanisms underlying its contribution remain unclear and further studies need to be performed to understand the role of *YWHAZ* in brain development and function.

YWHAZ is a member of the 14-3-3 gene family, coding for a highly conserved group of molecular chaperones that play important roles in biological processes and neuronal development [8]. *YWHAZ* encodes 14-3-3ζ, a protein involved in neurogenesis and neuronal migration as shown by morphological changes in the brain of 14-3-3ζ knockout mice [9–12]. These animals present behavioural and cognitive alterations that have been related to psychiatric disorders like schizophrenia [9, 12], including hyperactivity, impaired memory, lower anxiety and impaired sensorimotor gating.

A homologue of *YWHAZ* is also found in zebrafish, a species that represents a powerful model to study brain development and psychiatric disorders [13–15]. Zebrafish display well-defined behaviours that can be translated to humans in some cases [13, 15] and, although neurodevelopmental timings and brain organization differ between human and zebrafish, comparative studies have mapped these differences and the information gained in zebrafish can be transferred to other species [13, 16]. Importantly, zebrafish present high genetic homology to humans, are easy to manipulate genetically and their small size and transparency during larval stages make zebrafish ideal for *in vivo* imaging studies [13, 14]. Indeed, whole-brain imaging is a recently developed technique [17, 18] that allows *in vivo* assessment of neuronal activity and connectivity in zebrafish using light-sheet microscopy [19]. This novel approach, combined with genetic engineering, represents an excellent tool to study the neural mechanisms of human brain disorders in specific zebrafish models.

In this study, we aimed to understand the mechanisms by which *YWHAZ* contributes to the development of psychiatric disorders. We explored the effect of loss of *ywhaz* function on neural activity and connectivity during development, and in neurotransmission and behaviour during adulthood.

MATERIAL AND METHODS

Further details about the procedures are described in the Supplementary methods.

Zebrafish strains, care and maintenance

Adult zebrafish and larvae (*Danio rerio*) were maintained at 28.5°C on a 14:10 light-dark cycle following standard protocols. All experimental procedures were approved by a local Animal Welfare and Ethical Review board (University of Leicester and Generalitat de Catalunya). AB wild-type (WT), *Tg*(*aldoca:gap43-Venus*), *Tg*(*olig2*:*egfp*)^{vu12}, *ywhaz*$^{-/-}$, albino *Tg(elavl3:GCaMP6s)* and albino *Tg(elavl3:GCaMP6s) ywhaz*$^{-/-}$ zebrafish lines were used for the experiments.

Generation of *ywhaz* zebrafish knock out using CRISPR/Cas9

We used CRISPR/Cas9 to engineer a 7-bp frameshift deletion (380_387delCCTGGCA) within the third exon of *ywhaz* that leads to a premature stop codon in the third exon of the unique *ywhaz* isoform and generates an ORF that is 48% shorter than the normal one (Figure S1).

In situ hybridization (ISH) and immunohistochemistry (IHC)

A specific mRNA probe targeting *ywhaz* (NCBI Reference Sequence: NM_212757.2) was prepared and ISH experiments were performed in larvae and dissected adult brains of AB wild-type (WT), *Tg*(*aldoca:gap43-Venus*), *Tg*(*olig2*:*egfp*)^{vu12} and *ywhaz*$^{-/-}$ zebrafish strains. IHC was performed in adult *Tg*(*olig2*:*egfp*)^{vu12}, *ywhaz*$^{-/-}$ and *Tg*(*aldoca*:*gap43-Venus*)^{rk22} brains.

Gene expression analysis using Real-Time quantitative PCR (RT-qPCR)

Total RNA was extracted from the whole brains of WT and *ywhaz*$^{-/-}$ adult zebrafish and RT-qPCR was performed on 10 brains per genotype with three replicates.

Whole-brain imaging

Whole-brain imaging experiments were performed on 6 days-post-fertilization (dpf) albino *Tg(elavl3:GCaMP6s)* and *Tg(elavl3:GCaMP6s) ywhaz*$^{-/-}$ zebrafish larvae. Recordings were performed using a light sheet microscope, image segmentation and extraction of calcium signals were performed following the Caiman MATLAB pipeline [20] and Netcal was used to analyse activity and functional connectivity (www.itsnetcal.com) [21] (Figure 1).

High performance liquid chromatography (HPLC) analysis of monoamines and metabolites

Fish were decapitated and their brains were dissected and divided into four areas: telencephalon (Tel), diencephalon (DI), optic tectum (TeO) and hindbrain (Hb). HPLC analysis for dopamine (DA), serotonin (5-HT), 3,4-dihydroxyphenylacetic acid (DOPAC), and 5-hydroxyindoleacetic acid (5-HIAA) was carried out using HPLC with electrochemical detection [22].

Behavioural tests

A battery of behavioural tests was performed in three batches of adult zebrafish (3-5 months-old) mixed groups of both sexes. Two tests to assess social behaviour were also performed on juvenile (one month-old) zebrafish. All fish were genotyped, sized-matched and maintained in groups by genotype until the day of testing. A battery of behavioural tests was also performed in a batch of sex-differentiated adult zebrafish. Most of the measures were performed automatically with a tracking system, and when any measure was manually quantified, we used a blinding system so that the experimenter did not know the genotype of the fish that was being analysed.

Drug treatments

Fluoxetine 5 mg/L diluted in DMSO (Tocris #0927) was administered by immersion for 2 hours. Quinpirole 0.25-4 mg/L diluted in H_2O (Tocris #1061) was administered by immersion for 1 hour.

Statistical methods

Statistical analysis of RT-qPCR, HPLC and behavioural data were performed with GraphPad Prism 8. The data sets were assessed for normality using D'Agostino-Pearson and Shaphiro-Wilk normality test. Either a Mann-Whitney or an unpaired t-test with or without Welch's correction was performed to compare two groups, and a Kruskal-Wallis test was used to compare between multiple groups. Statistical analysis of the visually-mediated social preference test was performed by a two-way ANOVA (no repeated measures) with Tukey or Sidak post-hoc test. Statistical analysis of neuronal activity and functional connectivity consisted of unpaired t-test between genotypes for each area. When necessary, Holm-Sidak or Dunn corrections were performed for multiple comparisons.

RESULTS

ywhaz expression is pan-neuronal during development and restricted to the cerebellum in adults

We first performed a phylogenetic analysis and confirmed that the zebrafish *ywhaz* gene is the orthologue of the human *YWHAZ* gene, as ywhaz is the 14-3-3 zebrafish protein most closely related to the human YWHAZ protein (Figure S2). We ~~first~~ then investigated *ywhaz* gene expression in the developing brain using *in situ* hybridization (ISH). In three to nine days post-fertilization (dpf) WT larvae, *ywhaz* expression is widespread covering almost all brain areas, with a particularly strong signal in the cerebellum of whole mount embryos (Figure 2A). In contrast, in adult zebrafish *ywhaz* expression is restricted to the cerebellum. *ywhaz* RNA is present in the granule cell layer (GCL) of the valvula cerebelli (Va) and crista cerebellaris (CCe), in an area that appears to be the Purkinje cell layer (PCL) (Figure 2B).

We next combined *ywhaz* ISH with an anti-GFP antibody stain on adult brain sections of *Tg*(*aldoca:gap43-Venus*) [23] and *Tg*(*olig2*:*egfp*)^{vu12} [24] transgenic lines, to confirm that *ywhaz* is only expressed Purkinje cells, inhibitory neurons in the PCL. We found that *ywhaz* ISH staining overlaps GFP in the *Tg*(*aldoca:gap43-Venus*) line but not in the *Tg*(*olig2*:*egfp*)^{vu12} line, meaning that at adult stages *ywhaz* is expressed within Purkinje cells and not within eurydendroid cells, excitatory neurons that are situated ventrally to Purkinje cells [25] ~~at adult stages~~ (Figure 2C and D) [23, 24].

ywhaz deficiency alters spontaneous neuronal activity and functional connectivity in the hindbrain of larvae

The pan-neuronal expression pattern of *ywhaz* suggests that it may play a role during neural development. We generated a knockout line in zebrafish by using CRISPR/Cas9 genome engineering [26] and confirmed the lack of *ywhaz* expression by ISH and RT-qPCR (see Figures S2 and S3 and supplementary methods for details). We then performed whole-brain imaging *in vivo* at 6 dpf to investigate changes in neural circuit function and connectivity between the WT and *ywhaz*$^{-/-}$ genotypes (see Figure 1 for methodological details and Supplementary Videos 1-3).

We found an increased number of active neurons in medulla oblongata (MO) of *ywhaz*$^{-/-}$ fish ($p = 0.046$), which represents a higher fraction of total active neurons ($p = 0.005$) (Figure 3A). This relative increase of active neurons in the MO correlates with a significant decrease in active cerebellar neurons in *ywhaz*$^{-/-}$ fish ($p = 0.018$, Figure 3A). In thalamus and tegmentum, the low number of active neurons that we could detect prevented us from properly assessing activity and connectivity in these areas (Figure S4A).

Single-cell activity analysis (Figure S4B) showed that a lower fraction of total spikes was contained within single-cell bursts in the MO of *ywhaz*$^{-/-}$ fish ($p = 0.039$, Figure 3B). In addition, population-level analysis (Figure S5) showed that a lower fraction of neurons participated in large-scale bursts (defined as large increases in activity within an area) in the MO of *ywhaz*$^{-/-}$ fish ($p = 0.016$), and the average increase in activity during these bursts was also lower in MO and tectum in *ywhaz*$^{-/-}$ fish ($p = 0.006$ for MO and $p = 0.043$ for tectum) (Figure 3C). Finally, principal component analysis showed that for any target variance explained, *ywhaz*$^{-/-}$ always required a larger number of components, suggesting less coherence in the activity modes of *ywhaz*$^{-/-}$ in the MO ($p = 0.005$, Figure 3D). This effect was not found in other areas (Figure S6A).

We then explored possible alterations in functional connectivity inside each of the defined areas (Figure S6B). We found a higher clustering coefficient (relative number of loops in a network) ($p = 0.022$) and a higher global efficiency (a measure of how easy it is for activity to move throughout a network) ($p = 0.044$) in cerebellum of *ywhaz*$^{-/-}$ fish (Figure 3E). Also, we observed a higher assortativity (the correlation of the number of connections between connected neurons in a network) ($p = 0.001$) and a higher Louvain community statistic (a measure of how segregated the communities of a network are) in MO of *ywhaz*$^{-/-}$ fish ($p = 0.010$) (Figure 3E). Finally, analyses of connectivity distribution showed that in the MO of WT fish there is a subpopulation of highly connected neurons that is not present in the MO of *ywhaz*$^{-/-}$ fish (Figure 3F), but no differences were found in cerebellum and tectum (Figure S6B). These highly connected neurons in the MO of WT fish are likely to be responsible for connecting communities within a network together, resulting in a more coherent pattern of collective activity in WT fish, and their absence in *ywhaz*$^{-/-}$ fish would lead to an impairment of MO activity.

Altogether, these results show that in *ywhaz*$^{-/-}$ fish cerebellar neurons represent a lower fraction of total brain neurons but present a higher clustering and more effective connectivity. Also, the presence of more isolated neuronal communities in the MO of *ywhaz*$^{-/-}$ fish would generate a lower collective burst activity and synchrony in this area and would lead to an impaired MO activity.

ywhaz deficiency alters monoamine levels in adult hindbrain

Spontaneous synchronized neuronal communication plays an important role during early development in establishing the mature brain circuitry [27–30]. We therefore hypothesized that the alterations in neuronal spontaneous activity found in *ywhaz*$^{-/-}$ larvae may affect neuronal migration and wiring and have a long-term impact in neurotransmission in adults. We performed high performance liquid chromatography (HPLC) to measure the basal levels of several neurotransmitters and metabolites: 3,4-dihydroxyphenylacetic acid (DOPAC), dopamine (DA), 5-hydroxyindoleacetic acid (5HIAA) and serotonin (5-HT), in the brain of *ywhaz*$^{-/-}$ and WT adult fish. We found a significant reduction of DA and 5-HT levels in the hindbrain of *ywhaz*$^{-/-}$ ($p = 0.006$ and $p = 0.003$ respectively, Figure 4A). No further alterations were found in other areas of the brain (Figure S7A-C) nor in the breakdown of 5-HT to 5HIAA, or DA to DOPAC (Figure S7D-E).

Loss of _ywhaz_ function alters the expression of genes involved in the dopaminergic and serotonergic pathways

The reduced levels of DA and 5-HT in mutants suggests that *ywhaz* may influence the synthesis of these neurotransmitters. Tyrosine hydroxylase (TH) and Tryptophan hydroxylase (TPH), rate-limiting enzymes in the biosynthesis of DA and 5-HT, respectively, are known to be regulated by 14-3-3 proteins [31]. We therefore first quantified the expression of genes coding for the DA and 5-HT synthesis enzymes TH and TPH in adult fish. There was an increase in *tryptophan hydroxylase 2* (*tph2*) and *tyrosine* hydroxylase 1 (*th1*) expression in *ywhaz*$^{-/-}$ compared to WT, although differences in *th1* did not overcome testing for multiple corrections. *tph1a*, *tph1b* and *th2* showed all a low expression in both genotypes (Figure 4B). We further examined the transcription of genes coding for proteins involved in the dopaminergic neurotransmitter pathway: the dopamine transporter *solute carrier family 6 member 3* (*slc6a3*), *dopamine receptor 1* (*drd1*), *dopamine receptor 2a* (*drd2a*), *dopamine receptor 2b* (*drd2b*) and *dopamine* *receptor 4* (*drd4*). The expression of the two isoforms *drd2a and drd2b* was significantly increased in *ywhaz*$^{-/-}$ compared to WT (Figure 4C).

Monoaminergic drugs reverse *ywhaz*$^{-/-}$ freeze in response to novelty

We performed a battery of behavioural tests in adult WT and *ywhaz*$^{-/-}$ mutants to characterize possible alterations in behaviour due to *ywhaz* deficiency (Figure S8). We only found differences between genotypes in the visually-mediated social preference (VMSP) test, used to assess social behaviour. During the social preference step, both genotypes spent most of the time swimming close to the first group of strangers ($p < 0.0001$ for both WT and *ywhaz*$^{-/-}$; Figure S8D). However, during the preference for social novelty step, WT switched preference to the second group of unfamiliar fish ($p = 0.048$, Figure S8D) whereas *ywhaz*$^{-/-}$ fish did not show any preference ($p = 0.98$, Figure S8D). Instead, we found that immediately after the addition of the second group of unfamiliar fish, *ywhaz*$^{-/-}$ mutants froze significantly more than WT ($p = 0.004$; Figure 5A). We repeated the test by adding marbles instead of the second group of unfamiliar fish and observed the same freezing behaviour in response to novelty in *ywhaz*$^{-/-}$ mutants ($p = 0.025$, Figure 5B). Contrary to adults, juvenile *ywhaz*$^{-/-}$ fish did not show altered social behaviour: they did not show any increase in freezing behaviour in the VMSP test ($p > 0.99$, Figure S8F), nor an altered cluster score in the shoaling test for social interaction in a group (Figure S8G).

HPLC and qPCR results suggested that alterations in 5-HT and DA signalling may underlie the behavioural phenotype of *ywhaz*$^{-/-}$. We therefore used fluoxetine, a selective serotonin reuptake inhibitor (SSRI) [32], and quinpirole, a selective D2-like receptor agonist [33] to investigate the connection between 5-HT, DA, and the behavioural phenotype observed in *ywhaz*$^{-/-}$ in the VMSP test. Treatment with 5 mg/L fluoxetine and treatment with 0.25 mg/L quinpirole significantly decreased the time *ywhaz*$^{-/-}$ spent freezing after the addition of the second group of unfamiliar fish ($p = 0.006$ and $p = 0.047$, respectively, Figure 5C and D) without affecting WT behaviour. However, a higher concentration of quinpirole, 1 or 4 mg/L, did not reverse the freezing behaviour ($p > 0.99$ for both concentrations, Figure 5D).

Several behavioural tests were repeated in a second group of adult fish and increased freezing behaviour was observed in *ywhaz*$^{-/-}$ fish in all the tests performed (Figure S9A). Additionally, a third batch of behavioural tests was performed in a different setup, but strong differences in the WT behaviour of this batch, probably due to environmental effects, prevented us from comparing the results obtained in this batch with the previous batches (Figure S9B).

We also investigated the influence of sex on locomotion and social behaviour separating the fish by sex (Figures S10 and S11). We observed differences between WT and *ywhaz*$^{-/-}$ females in social behaviour, as WT females present a lower nearest neighbour distance (NND) and interindividual distance (IID) in the shoaling test (Figure S10) and spend more time close to the 1st strangers in the social preference step of the VMSP test than *ywhaz*$^{-/-}$ females (Figure S11). No differences were observed between WT and *ywhaz*$^{-/-}$ males, and between *ywhaz*$^{-/-}$ males and females. However, differences were observed in shoaling behaviour between WT males and WT females: WT females swim shorter distances, display a lower speed and stay closer to the other members of the shoal compared to males (Figure S10).

DISCUSSION

Functional and genetic studies had previously suggested a role for the *YWHAZ* gene in neurodevelopmental disorders such as ASD or schizophrenia [2, 3, 9, 12]. In this study, we have used zebrafish to investigate *ywhaz* function in neural development and behaviour, showing that *in vivo* whole-brain imaging is a powerful tool to understand the mechanisms involved in brain disorders. We found that *ywhaz* deficiency resulted in an altered hindbrain connectivity during larval stages and a neurotransmitter imbalance during adulthood leading to freezing in response to novelty.

We observed a pan-neuronal expression of *ywhaz* in larval stages, which suggests that *ywhaz* may be involved in a wide range of functions during zebrafish neurodevelopment. The important function of *Ywhaz* in neurogenesis and neuronal differentiation was previously demonstrated in mice KO models [8–12], and disrupted neurogenesis is a known risk factor for neurodevelopmental disorders [34]. Although expressed pan-neuronally, *ywhaz* presents a stronger expression in larvae cerebellum, a brain region whose dysfunction has been related to neurodevelopmental disorders [35, 36]. Interestingly, decreased *YWHAZ* expression was reported in the cerebellum of ASD patients [2]. In adult zebrafish, *ywhaz* is specifically expressed in Purkinje cells (PC) in the cerebellum. *Postmortem* studies have shown a reduction in PC number, size and density in the brain of autistic patients [37–40], and *Tsc1* mutant mice with a decrease in PC functioning show autistic-like behaviours [41]. *ywhaz* is therefore expressed in brain regions that play a crucial role in neurodevelopment and whose dysfunction is related to neurodevelopmental disorders.

Spontaneous bursting activity during development is essential for the correct assembly of neural circuits [27, 42]. This activity has been shown to control apoptosis and future connectivity in the developing cortex of mice [43], and in the larval zebrafish optic tectum it is involved in the processing of sensory information [28]. In addition, resting state magnetic resonance studies have revealed an altered spontaneous functional connectivity in patients diagnosed with ASD or schizophrenia [44–48]. Here, *ywhaz*$^{-/-}$ larvae present decreased burst activity and synchronization in the hindbrain, the region where *ywhaz* showed a higher expression in WT animals. These results together with the observed decreased levels of DA and 5-HT in the hindbrain of *ywhaz*$^{-/-}$ adults point to long-term alterations in brain function. These findings suggest that *ywhaz* is involved in establishing brain connectivity during development and that this impaired connectivity may contribute to the subsequent neurotransmitter imbalance found in adults.

Among all 14-3-3 isoforms, *YWHAZ* plays the most important role in DA synthesis [49]. *YWHAZ* is known to regulate the function of TH and TPH, rate-limiting enzymes in the biosynthesis of DA and 5-HT [31]. In previous work, we demonstrated that a disrupting mutation in *YWHAZ* produces a loss of affinity of the protein for TH [2]. Therefore, *ywhaz* deficiency may contribute to a decrease in TH activity and a subsequent reduction in DA levels. These results are in line with the alterations in the DA system previously reported in patients with neurodevelopmental disorders such as ASD, ADHD or schizophrenia [50–52]. The increased *drd2a* and *drd2b* levels we reported in *ywhaz* mutants may be due to compensatory mechanisms to overcome DA depletion. Interestingly, schizophrenia patients have a higher density of DRD2 receptors and all antipsychotic drugs used today are DRD2 antagonists [53, 54]. In addition, upregulation of *tph2* may be a mechanism to compensate for the depletion of 5-HT we found in the hindbrain of *ywhaz*$^{-/-}$ adults. In line with these results, altered levels of 5-HT have been reported in ASD and schizophrenia patients [55, 56]. Finally, we analysed the expression levels of *ywhae* in adult *ywhaz*$^{-/-}$ brains, another member of the 14-3-3 gene family that forms hetorodimers with *ywhaz.* Although the differences are not significant and a further study is needed, we hypothesize that upregulation of other 14-3-3 proteins may compensate for some aspects of *ywhaz* depletion.

Treatment with fluoxetine, a serotonin reuptake inhibitor, and quinpirole, a selective DRD2-like receptor agonist, was able to rescue the abnormal neophobic freezing behaviour observed in *ywhaz* mutants. Similarly, in a previous study, behavioural alterations were rescued in *Ywhaz*$^{-/-}$ mice using the antipsychotic drug clozapine, an antagonist of DA and 5-HT receptors used as a medication for schizophrenia [57]. In addition, several studies have shown a significant decrease in the frequency and intensity of restrictive and repetitive behaviours in ASD patients treated with fluoxetine. However, other autistic symptoms were not significantly improved by fluoxetine treatments (reviewed in [58]). 5-HT and DA are involved in sensory processing and social cognition [59, 60], and DA plays an important role in social reward [61]. Given the function of 5-HT and DA in behaviour, we hypothesize that the alterations to 5-HT and DA signalling in mutant fish are responsible for the exaggerated response to novel stimuli present in *ywhaz*$^{-/-}$ adults.

Several sex differences were found in social behaviour when exploring behaviour in females and males separately. WT females show a lower locomotor activity and swim closer to each other in the shoaling test compared to WT males. In addition, alterations of social behaviour due to the *ywhaz*$^{-/-}$ genotype were only reported in the case of females. These results are in line with sex-related differences reported in neurodevelopmental and psychiatric disorders in humans [62] and highlight the importance of taking sex into account when investigating psychiatric conditions. However, further research is still needed to better understand the underlying genetic and hormonal influences of these sex-related behavioural differences.

Certain strengths and limitations of this study should be discussed. First, whole-brain imaging experiments were performed in 6 dpf larvae whereas neurotransmitter levels and behaviour were investigated in adult fish due to the impossibility of performing all these experiments at the same age. Even though this constitutes a limitation, it brings useful complementary information to analyse the effect of *ywhaz* deficiency at different levels and ages. In addition, our whole-brain imaging setup did not permit us to analyse neuronal activity in ventral telencephalic and diencephalic brain regions like the ventral thalamus and hypothalamus, where important DA and 5-HT nuclei are located. Finally, the differences observed in the behavioural phenotype between batches of experiments may be due to environmental differences (between setups) and to (epi)genetic changes between fish generations. Indeed, a previous study reported differences between *Ywhaz*$^{-/-}$ mice with a different genetic background [9], and it is well described that environment plays an important role in the onset or phenotypical expression of psychiatric and neurodevelopmental disorders.

In conclusion, our findings highlight the important role of *YWHAZ* in neurodevelopment and shed light on the neurobiological mechanisms underlying its contribution to neurodevelopmental disorders. In addition, this work highlights the use of whole-brain imaging techniques as a promising approach for the study of neurodevelopmental disorders as it provides valuable and precise information about the mechanisms underlying the observed phenotype. Finally, pharmacological rescue of altered behaviour of *ywhaz*$^{-/-}$ fish provide some clues for the use of specific treatments to revert the associated symptomatology in neuropsychiatric disorders such as ASD or schizophrenia.

AUTHORS CONTRIBUTION

N.F-C, WHJ.N and B.C. conceived and coordinated the study, N.F-C. designed the experimental approaches for whole-brain imaging, WHJ.N designed the behavioural and pharmacological approaches and B.C. designed the genetic approaches. E.A-G. designed and conducted the whole-brain imaging and behavioural experiments and wrote the paper, E.DV. designed and conducted the CRISPR/Cas9, ISH, IHC, HPLC and behavioural experiments. AMJ.Y. contributed to the HPLC experiments. C.H-U. and J.G-F. carried out the phylogenetic analysis. M.G-P contributed to the behavioural experiments. C.A. contributed to the statistical analysis of the behavioural tests. JG.O. designed the pipeline and methodology for the whole-brain imaging analyses, G.C. and E.G. conducted the whole-brain imaging recordings, E.A-G. analyzed the imaging data, F.A. contributed to the whole-brain imaging analysis and P.L-A supervised the whole-brain imaging recordings. All authors discussed and commented on the manuscript.

ACKNOWLEDGEMENTS

GCaMP6s albino zebrafish embryos were generated by the National Institute of Genetics (Japan) and obtained from Dr. Matt Parker from the University of Portsmouth, UK. The *Tg(aldoca:gap43-Venus)* line was obtained from Masahiko Hibi from the Bioscience and Biotechnology Center of Nagoya University, Japan. *Tg(olig2:egfp)*^{vu12} brains were obtained from the Center for Developmental Biology, UMR 5547 CNRS, Toulouse, France. Major financial support for this research was received by BC from the Spanish 'Ministerio de Ciencia, Innovación y Universidades' (RTI2018-100968-B-100, PID2021-1277760B-I100), the 'Ministerio de Sanidad, Servicios Sociales e Igualdad/Plan Nacional Sobre Drogas' (PNSD-2017I050 and PNSD-2020I042), 'Generalitat de Catalunya/AGAUR' (2017-SGR-738), ICREA Academia 2021, and the European Union H2020 Program [H2020/2014-2020] under grant agreements n° 667302 (CoCA) and Eat2beNICE (728018). E.A-G was supported by the Ministerio de Economía y Competitividad (Spanish Government) and the EU H2020 program (Eat2beNICE-728018). G.C., E.G. and P.L-A acknowledge financial support from the Spanish Ministerio de Economía y Competitividad (MINECO) through the "Severo Ochoa" program for Centres of Excellence in R&D CEX2019-000910-S), MINECO/FEDER Ramon y Cajal program (RYC-2015-17935); Laserlab-Europe EU-H2020 GA no. 871124, Fundació Privada Cellex, Fundación Mig-Puig and from the Generalitat de Catalunya through the CERCA program. F.A. acknowledges financial support from the Spanish

‘Ministerio de Ciencia, Innovación y Universidades’ (PID2019-107738RB-I00, MICINN/FEDER) and SGR (2017SGR1255).

CONFLICT OF INTEREST

The authors declare no conflict of interest.

Supplementary information is available at MP’s website.

REFERENCES

1. Jia Y, Yu X, Zhang B, Yuan Y, Xu Q, Shen Y, et al. An association study between polymorphisms in three genes of 14-3-3 (tyrosine 3-monooxygenase/tryptophan 5-monooxygenase activation protein) family and paranoid schizophrenia in northern Chinese population. Eur Psychiatry. 2004;19:377–379.

2. Torrico B, Antón-Galindo E, Fernàndez-Castillo N, Rojo-Francàs E, Ghorbani S, Pineda-Cirera L, et al. Involvement of the 14-3-3 Gene Family in Autism Spectrum Disorder and Schizophrenia: Genetics, Transcriptomics and Functional Analyses. J Clin Med. 2020;9:1851.

3. Toma C, Torrico B, Hervás A, Valdés-Mas R, Tristán-Noguero A, Padillo V, et al. Exome sequencing in multiplex autism families suggests a major role for heterozygous truncating mutations. Mol Psychiatry. 2014;19:784–790.

4. Middleton FA, Peng L, Lewis DA, Levitt P, Mirnics K. Altered expression of 14-3-3 in the prefrontal cortex of subjects with schizophrenia. Neuropsychopharmacology. 2005;30:974–983.

5. English JA, Pennington K, Dunn MJ, Cotter DR. The neuroproteomics of schizophrenia. Biol Psychiatry. 2011;69:163–172.

6. Pagan C, Delorme R, Callebert J, Goubran-Botros H, Amsellem F, Drouot X, et al. The serotonin-N-acetylserotonin-melatonin pathway as a biomarker for autism spectrum disorders. Transl Psychiatry. 2014;4:e479.

7. Pagan C, Goubran-Botros H, Delorme R, Benabou M, Lemière N, Murray K, et al. Disruption of melatonin synthesis is associated with impaired 14-3-3 and miR-451 levels in patients with autism spectrum disorders. Sci Rep. 2017;7:2096.

8. Cornell B, Toyo-oka K. 14-3-3 proteins in brain development: Neurogenesis, neuronal migration and neuromorphogenesis. Front Mol Neurosci. 2017;10:318.

9. Xu X, Jaehne EJ, Greenberg Z, McCarthy P, Saleh E, Parish CL, et al. 14-3-3ζ deficient mice in the BALB/c background display behavioural and anatomical defects associated with neurodevelopmental disorders. Sci Rep. 2015;5:12434.

10. Toyo-Oka K, Wachi T, Hunt RF, Baraban SC, Taya S, Ramshaw H, et al. 14-3-3E and Z Regulate Neurogenesis and Differentiation of Neuronal Progenitor Cells in the Developing Brain. J Neurosci. 2014;34:12168–12181.

11. Jaehne EJ, Ramshaw H, Xu X, Saleh E, Clark SR, Schubert KO, et al. In-vivo administration of clozapine affects behaviour but does not reverse dendritic spine deficits in the 14-3-3ζ KO mouse model of schizophrenia-like disorders. Pharmacol Biochem Behav. 2015;138:1–8.

12. Cheah PS, Ramshaw HS, Thomas PQ, Toyo-Oka K, Xu X, Martin S, et al. Neurodevelopmental and neuropsychiatric behaviour defects arise from 14-3-3ζ deficiency. Mol Psychiatry. 2012;17:451–466.

13. Kalueff A V., Stewart AM, Gerlai R. Zebrafish as an emerging model for studying complex brain disorders.

Trends Pharmacol Sci. 2014;35:63–75.

14. Norton W. Towards developmental models of psychiatric disorders in zebrafish. Front Neural Circuits. 2013;7:79.

15. Vaz R, Hofmeister W, Lindstrand A. Zebrafish models of neurodevelopmental disorders: Limitations and benefits of current tools and techniques. Int J Mol Sci. 2019;20:1296.

16. Kozol RA, Abrams AJ, James DM, Buglo E, Yan Q, Dallman JE. Function over form: Modeling groups of inherited neurological conditions in zebrafish. Front Mol Neurosci. 2016;9:55.

17. Ahrens MB, Orger MB, Robson DN, Li JM, Keller PJ. Whole-brain functional imaging at cellular resolution using light-sheet microscopy. Nat Methods. 2013;10:413–420.

18. Vanwalleghem GC, Ahrens MB, Scott EK. Integrative whole-brain neuroscience in larval zebrafish. Curr Opin Neurobiol. 2018;50:136–145.

19. Olarte OE, Andilla J, Gualda EJ, Loza-Alvarez P. Light-sheet microscopy : a tutorial. Adv Opt Photonics. 2018;10:111–179.

20. Giovannucci A, Friedrich J, Gunn P, Kalfon J, Brown BL, Koay SA, et al. CaImAn an open source tool for scalable calcium imaging data analysis. Elife. 2019;8:e38173.

21. Orlandi JG, Fernández-García S, Comella-Bolla A, Masana M, Barriga GG-D, Yaghoubi M, et al. NETCAL: An interactive platform for large-scale, NETwork and population dynamics analysis of CALcium imaging recordings (7.0.0 Open Beta). Zenodo. 2017:10.5281/zenodo.1119026.

22. Young AMJ. Increased extracellular dopamine in nucleus accumbens in response to unconditioned and conditioned aversive stimuli: Studies using 1 min microdialysis in rats. J Neurosci Methods. 2004;138:57–63.

23. Ahn AH, Dziennis S, Hawkes R, Herrup K. The cloning of zebrin II reveals its identity with aldolase C. Development. 1994;120:2081–2090.

24. McFarland KA, Topczewska JM, Weidinger G, Dorsky RI, Appel B. Hh and Wnt signaling regulate formation of olig2+ neurons in the zebrafish cerebellum. Dev Biol. 2008;318:162–171.

25. Biechl D, Dorigo A, Köster RW, Grothe B, Wullimann MF. Eppur Si muove: Evidence for an external granular layer and possibly transit amplification in the teleostean cerebellum. Front Neuroanat. 2016;10:49.

26. Kai W, Kunwar KC J, Elisa DV, Sunil P, Norbert G, Anne D, et al. Cysteine modification by ebselen reduces the stability and cellular levels of 14-3-3 proteins. Mol Pharmacol. 2021;100:155–169.

27. Molnár Z, Luhmann HJ, Kanold PO. Transient cortical circuits match spontaneous and sensory-driven activity during development. Science (80-). 2020;370:eabb2153.

28. Marachlian E, Avitan L, Goodhill GJ, Sumbre G. Principles of functional circuit connectivity: Insights from spontaneous activity in the zebrafish optic tectum. Front Neural Circuits. 2018;12:46.

29. Avitan L, Pujic Z, Mölter J, Van De Poll M, Sun B, Teng H, et al. Spontaneous Activity in the Zebrafish Tectum Reorganizes over Development and Is Influenced by Visual Experience. Curr Biol. 2017;27:2407-2419.e4.

30. Momose-Sato Y, Sato K. Development of spontaneous activity in the avian hindbrain. Front Neural Circuits. 2016;10:63.

31. Aitken A. 14-3-3 proteins: A historic overview. Semin Cancer Biol. 2006;16:162–172.

32. Vaswani M, Linda FK, Ramesh S. Role of selective serotonin reuptake inhibitors in psychiatric disorders: A comprehensive review. Prog Neuro-Psychopharmacology Biol Psychiatry. 2003;27:85–102.

33. Millan MJ, Maiofiss L, Cussac D, Audinot V, Boutin JA, Newman-Tancredi A. Differential actions of antiparkinson agents at multiple classes of monoaminergic receptor. I. A multivariate analysis of the binding profiles of 14 drugs at 21 native and cloned human receptor subtypes. J Pharmacol Exp Ther. 2002;303:791–804.

34. Packer A. Neocortical neurogenesis and the etiology of autism spectrum disorder. Neurosci Biobehav Rev. 2016;64:185–195.

35. Stoodley CJ. The Cerebellum and Neurodevelopmental Disorders. Cerebellum. 2016;15:34–37.

36. van der Heijden ME, Gill JS, Sillitoe R V. Abnormal Cerebellar Development in Autism Spectrum Disorders. Dev Neurosci. 2021;43:181–190.

37. Fatemi SH, Halt AR, Realmuto G, Earle J, Kist DA, Thuras P, et al. Purkinje Cell Size Is Reduced in Cerebellum

of Patients with Autism. Cell Mol Neurobiol. 2002;22:171–175.

38. Palmen SJMC, van Engeland H, Hof PR, Schmitz C. Neuropathological findings in autism. Brain. 2004;127:2572–2583.

39. Bailey A, Luthert P, Dean A, Harding B, Janota I, Montgomery M, et al. A clinicopathological study of autism. Brain. 1998;121:889–905.

40. Skefos J, Cummings C, Enzer K, Holiday J, Weed K, Levy E, et al. Regional Alterations in Purkinje Cell Density in Patients with Autism. PLoS One. 2014;9:e81255.

41. Tsai PT, Hull C, Chu Y, Greene-Colozzi E, Sadowski AR, Leech JM, et al. Autistic-like behaviour and cerebellar dysfunction in Purkinje cell Tsc1 mutant mice. Nature. 2012;488:647–651.

42. Kirkby LA, Sack GS, Firl A, Feller MB. A role for correlated spontaneous activity in the assembly of neural circuits. Neuron. 2013;80:1129–1144.

43. Blanquie O, Yang JW, Kilb W, Sharopov S, Sinning A, Luhmann HJ. Electrical activity controls area-specific expression of neuronal apoptosis in the mouse developing cerebral cortex. Elife. 2017;6:e27696.

44. O'Reilly C, Lewis JD, Elsabbagh M. Is functional brain connectivity atypical in autism? A systematic review of EEG and MEG studies. PLoS One. 2017;12:e0175870.

45. Rane P, Cochran D, Hodge SM, Haselgrove C, Kennedy DN, Frazier JA. Connectivity in Autism: A Review of MRI Connectivity Studies. Harv Rev Psychiatry. 2015;23:223–244.

46. Li X, Zhang K, He X, Zhou J, Jin C. Structural, Functional, and Molecular Imaging of Autism Spectrum Disorder. Neurosci Bull. 2021;37:1051–1071.

47. Sheffield JM, Barch DM. Cognition and resting-state functional connectivity in schizophrenia. Neurosci Biobehav Rev. 2016;61:108–120.

48. Van Den Heuvel MP, Fornito A. Brain networks in schizophrenia. Neuropsychol Rev. 2014;24:32–48.

49. Wang J, Lou H, Pedersen CJ, Smith AD, Perez RG. 14-3-3ζ contributes to tyrosine hydroxylase activity in MN9D cells: Localization of dopamine regulatory proteins to mitochondria. J Biol Chem. 2009;284:14011–14019.

50. Kesby JP, Eyles DW, McGrath JJ, Scott JG. Dopamine, psychosis and schizophrenia: The widening gap between basic and clinical neuroscience. Transl Psychiatry. 2018;8:30.

51. Pavăl D. A Dopamine Hypothesis of Autism Spectrum Disorder. Dev Neurosci. 2017;39:355–360.

52. Tripp G, Wickens JR. Neurobiology of ADHD. Neuropharmacology. 2009;57:579–589.

53. Zakzanis KK, Hansen KT. Dopamine D2 densities and the schizophrenic brain. Schizophr Res. 1998;32:201–206.

54. Kestler LP, Walker E, Vega EM. Dopamine receptors in the brains of schizophrenia patients: A meta-analysis of the findings. Behav Pharmacol. 2001;12:355–371.

55. Gabriele S, Sacco R, Persico AM. Blood serotonin levels in autism spectrum disorder: A systematic review and meta-analysis. Eur Neuropsychopharmacol. 2014;24:919–929.

56. Muck-Seler D, Pivac N, Mustapic M, Crncevic Z, Jakovljevic M, Sagud M. Platelet serotonin and plasma prolactin and cortisol in healthy, depressed and schizophrenic women. Psychiatry Res. 2004;127:217–226.

57. Ramshaw H, Xu X, Jaehne EJ, McCarthy P, Greenberg Z, Saleh E, et al. Locomotor hyperactivity in 14-3-3ζ KO mice is associated with dopamine transporter dysfunction. Transl Psychiatry. 2013;3:e327.

58. Persico AM, Ricciardello A, Lamberti M, Turriziani L, Cucinotta F, Brogna C, et al. The pediatric psychopharmacology of autism spectrum disorder: A systematic review - Part I: The past and the present. Prog Neuro-Psychopharmacology Biol Psychiatry. 2021;110:110326.

59. Jacob SN, Nienborg H. Monoaminergic Neuromodulation of Sensory Processing. Front Neural Circuits. 2018;12:51.

60. Fernández M, Mollinedo-Gajate I, Peñagarikano O. Neural Circuits for Social Cognition: Implications for Autism. Neuroscience. 2018;370:148–162.

61. Rademacher L, Schulte-Rüther M, Hanewald B, Lammertz S. Reward: From basic reinforcers to anticipation of social cues. Curr Top Behav Neurosci. 2016;30:207–221.

62. Franceschini A, Fattore L. Gender-specific approach in psychiatric diseases: Because sex matters. Eur J Pharmacol. 2021;896:173895.

FIGURE LEGENDS

Figure 1. Whole-brain imaging methods. (A) Steps followed to perform the whole-brain imaging recordings in 6 days post-fertilization (dpf) larvae expressing GCaMP6s pan-neuronally. First, multiple crossings were performed between the *Tg*(*elavl3:GCaMP6s*) and *ywhaz*$^{-/-}$ mutant lines in order to obtain *ywhaz*-deficient albino larvae expressing GCaMP6s pan-neuronally. Then, *Tg*(*elavl3:GCaMP6s*) *ywhaz*$^{-/-}$ and *Tg*(*elavl3:GCaMP6s*) *ywhaz*$^{+/+}$ 6 dpf larvae were paralysed with α-bungarotoxine and placed in a plastic tube to perform the whole-brain imaging recordings with a light-sheet microscope. (B) Steps followed in the single-cell fluorescence traces extraction. First, a mask was applied to each single plane to avoid detection of fluorescence outside the brain. Then, single-cell fluorescence traces were extracted for all the neurons detected in each single plane and combined to obtain neuronal activity from the whole-brain of each individual during the 20 min recording. Finally, brain regions were manually defined in order to analyse them separately. On the right, plots of all the neurons detected in each brain area of one individual. In a first approach, we divided the three largest regions (Ce, OT, and MO) by hemispheres and obtained no differences in the number of neurons or activity between hemispheres. Ce, cerebellum; MO, medulla oblongata; OT, optic tectum; ROI, region of interest; Te, tegmentum; Th, thalamus. (C) Three levels of analysis were performed in each of the five defined brain areas: single-cell activity, collective burst activity, and functional connectivity.

Figure 2. *ywhaz* mRNA is widely expressed during zebrafish development but restricted to the Purkinje cells in the cerebellum in adults. (A) *In situ* hybridization (ISH) using a *ywhaz* RNA probe (purple) of 3-9 days post-fertilization (dpf) WT zebrafish embryos shows that *ywhaz* expression is widespread covering almost all brain areas, with a strongest signal in cerebellum. On the left, a whole-mount of a 3 dpf embryo. On the right, coronal sections of 3, 6 and 9 dpf embryos, including the MO and CeP brain areas. (B) Coronal and sagittal sections of WT adult brains after ISH with a *ywhaz* RNA probe (purple) shows that in WT adult brains, *ywhaz* expression is restricted to the granule cell layer in the cerebellum. (C) Co-staining of the adult *Tg(aldoca:gap43-Venus)* cerebellum with a *ywhaz* riboprobe (purple) by ISH and anti-GFP antibody (brown) by immunohistochemistry (IHC) on a sagittal section. The overlap between the two staining (black arrows) indicates that *ywhaz* is localised within Purkinje cells. (D) Co-staining of the adult *Tg*(*olig2*:*egfp*)^{vu12} cerebellum with a *ywhaz* riboprobe (purple) by ISH and anti-GFP

antibody (brown) by IHC on a sagittal section. The absence of overlap between the two stains shows that *ywhaz* mRNA is not localized in eurydendroid cells. CCe, corpus cerebelli; CeP, cerebellar plate; LCa, lobus caudalis cerebelli; MO, medulla oblongata; Val, lateral valvula cerebelli; Vam, medial valvula cerebelli.

Figure 3. Decreased coherence in neuronal activity and decreased connectivity in the hindbrain of zebrafish *ywhaz*$^{-/-}$ larvae. (A) Number of active neurons and fraction of total active neurons detected in each brain area. (B) Fraction of total spikes participating in single-cell bursts in each brain area. (C) Fraction of total cells participating in collective bursts and burst amplitude in each brain area. Burst amplitude is measured as the increase of spikes (events) per second compared to basal spike activity. (D) Principal component analysis of the neuronal activity in the medulla oblongata (MO). (E) Normalized clustering coefficient, global efficiency, assortativity and Louvain community statistic in each brain area. (F) Connectivity distribution in the medulla oblongata (MO) of WT and *ywhaz*$^{-/-}$ larvae. A subpopulation of highly connected neurons exists in the MO of WT larvae that is absent in *ywhaz*$^{-/-}$ larvae. For A, B, C and E datasets: unpaired t-tests without Welch's correction. Each single point represents an individual, the central line represents the mean, the coloured darker shadow represents the 95% confidence interval and the lighter shadow the standard deviation (SD). For D and F: the central line represents the mean and the coloured shadow represents the 95% confidence interval. WT, wild-type larvae. n= 10 WT and 9 *ywhaz*$^{-/-}$. * $p < 0.05$, ** $p < 0.01$, *** $p < 0.001$.

Figure 4. Alterations in the monoamine neurotransmission in the hindbrain of adult KO. (A) High performance liquid chromatography in the hindbrain of WT and *ywhaz*$^{-/-}$ adult zebrafish. DA and 5-HT levels are decreased in the hindbrain of *ywhaz*$^{-/-}$ compared to WT. DA, dopamine; DOPAC, 3,4-dihydroxyphenylacetic acid; 5-HIAA, 5-hydroxyindoleacetic acid; 5-HT, 5-hydroxytryptamine. n = 7 WT, n = 7 ywhaz$^{-/-}$. (B) Relative expression profile of *tyrosine hydroxylase 1* (*th1*), *tyrosine hydroxylase 2* (*th2*), *tryptophan hydroxylase 1a* (*tph1a*), *tryptophan hydroxylase 1b* (*tph1b*) and *tryptophan hydroxylase* 2 (*tph2*), normalised to the reference gene ribosomal protein L13 (*rpl13*). *ywhaz*$^{-/-}$ fish have an increased level of *tph2* expression. n = 10 WT, n = 10 *ywhaz*$^{-/-}$. (C) Relative expression profile of the neurotransmitter transporter *solute carrier family 6 member 3* (*slc6a3*) and dopamine receptors *dopamine receptor 1* (*drd1*), *dopamine receptor 2a* (*drd2a*), *dopamine receptor 2b* (*drd2b*) and *dopamine receptor 4* (*drd4*), normalised to the reference gene *elongation factor 1a* (*elf1a*). *ywhaz*$^{-/-}$ have an increased level of *drd2a* and *drd2b* expression. n = 10 WT, n = 10 *ywhaz*$^{-/-}$. For all analyes: unpaired t-tests with

Welch’s correction and with Holm-Sidak correction for multiple comparisons. * $p < 0.05$. In all analyses plotted: mean ± SD.

Figure 5. Treatment with fluoxetine and quinpirole reverses the freezing behaviour observed in *ywhaz*$^{-/-}$ mutants. (A and B) Time spent freezing during the first two minutes after the addition of the second group of strangers (A) or marbles (B) in the behavioural setup during the second step of the visually mediated social preference test. Strangers: Unpaired t-test with Welch's correction; n = 12/genotype. Marbles: Mann-Whitney U test; n = 10/genotype. (C and D) Treatment with 5 mg/L fluoxetine and 0.25 mg/L quinpirole rescues the freezing phenotype in *ywhaz*$^{-/-}$. (C) Time spent freezing after the addition of the second group of unfamiliar fish in the tank with WT or *ywhaz*$^{-/-}$ fish treated with 5 mg/L fluoxetine or DMSO. Unpaired t-tests with Welch’s correction and with Holm-Sidak correction for multiple comparisons. n = 5 WT, n = 8 *ywhaz*$^{-/-}$. (D) Time spent freezing after the addition of the second group of unfamiliar fish in the tank with WT or *ywhaz*$^{-/-}$ fish treated with different concentrations of quinpirole. Kruskal-Wallis test with Dunn's multiple comparisons. n = 5 WT and n = 10 *ywhaz*$^{-/-}$ for Ctrl, 0.25 mg/L and 1 mg/L; and n = 5 *ywhaz*$^{-/-}$ for 4 mg/L. * $p < 0.05$, ** $p < 0.01$. In all analyses plotted: mean ± SD.

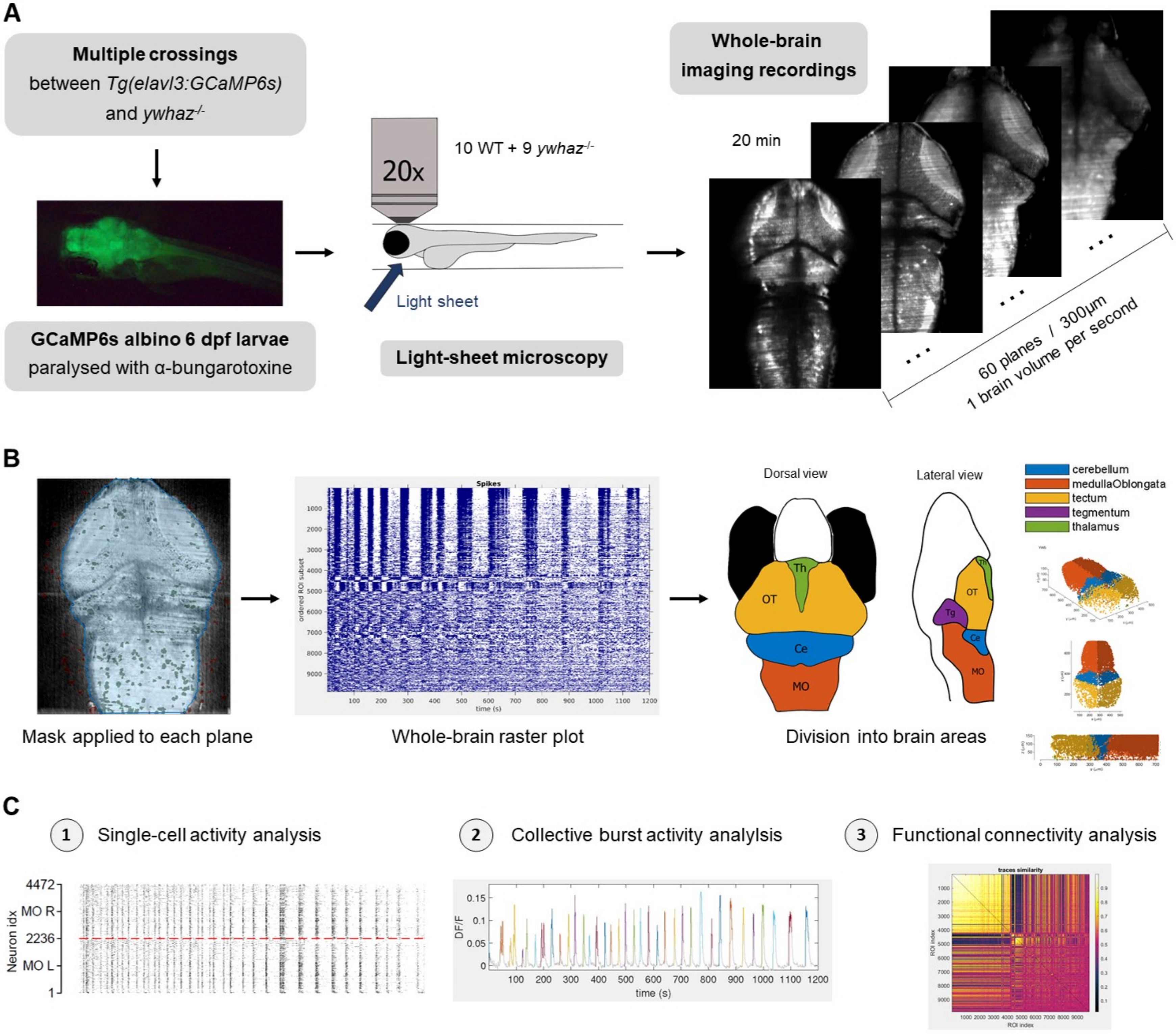

A
Multiple crossings
between Tg(elavl3:GCaMP6s)
and ywhaz-/-
GCaMP6s albino 6 dpf larvae
paralysed with α-bungarotoxine
20x
10 WT + 9 ywhaz-/-
Light sheet
Light-sheet microscopy
Whole-brain
imaging recordings
20 min
60 planes / 300µm
1 brain volume per second
B
Mask applied to each plane
Spikes
ordered ROI subset
time (s)
Whole-brain raster plot
Dorsal view
Lateral view
Th
OT
Ce
MO
Tg
cerebellum
medullaOblongata
tectum
tegmentum
thalamus
Division into brain areas
C
1 Single-cell activity analysis
2 Collective burst activity analysis
3 Functional connectivity analysis
Neuron idx
4472
MO R
2236
MO L
1
DF/F
time (s)
traces similarity
ROI index

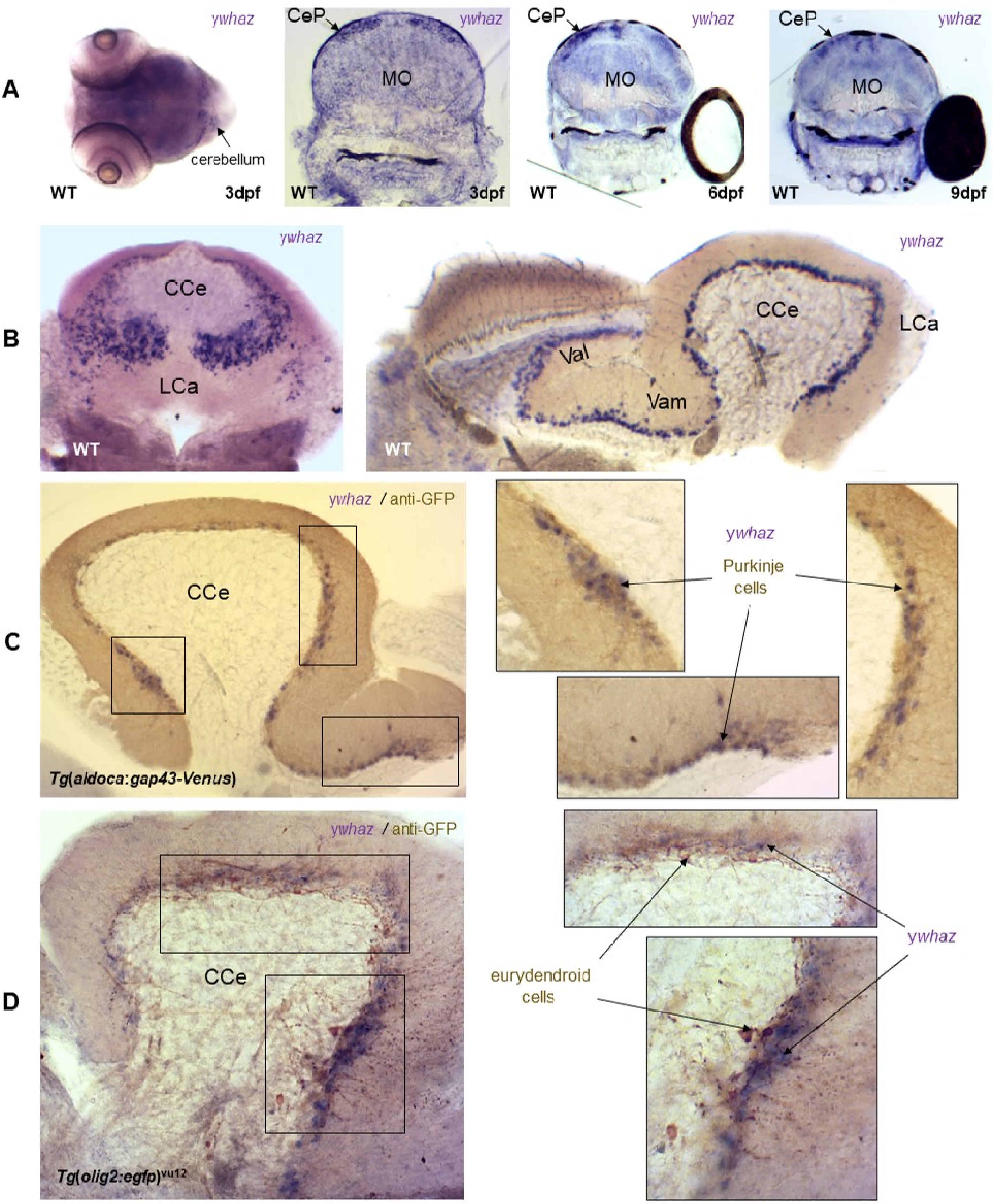
A
ywhaz
cerebellum
WT
3dpf
CeP
MO
6dpf
9dpf
B
CCe
LCa
Val
Vam
C
ywhaz / anti-GFP
Tg(aldoca:gap43-Venus)
Purkinje cells
D
Tg(olig2:egfp)vu12
eurydendroid cells

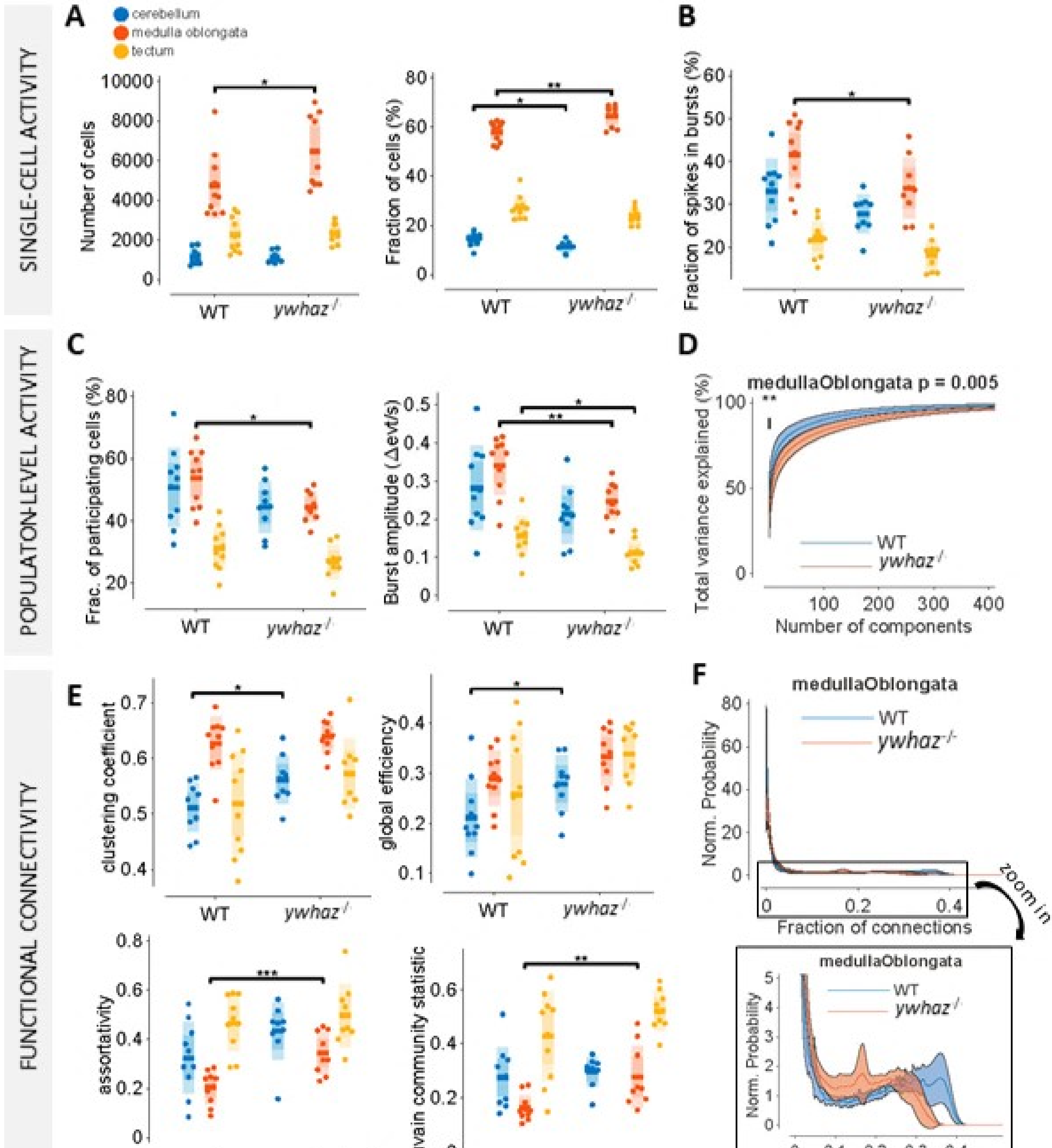
SINGLE-CELL ACTIVITY
POPULATON-LEVEL ACTIVITY
FUNCTIONAL CONNECTIVITY
A
cerebellum
medulla oblongata
tectum
Number of cells
Fraction of cells (%)
B
Fraction of spikes in bursts (%)
C
Frac. of participating cells (%)
Burst amplitude (Δevt/s)
D
medullaOblongata p = 0.005
Total variance explained (%)
Number of components
E
clustering coefficient
global efficiency
assortativity
louvain community statistic
F
medullaOblongata
Norm. Probability
Fraction of connections
zoom in
WT
ywhaz-/-

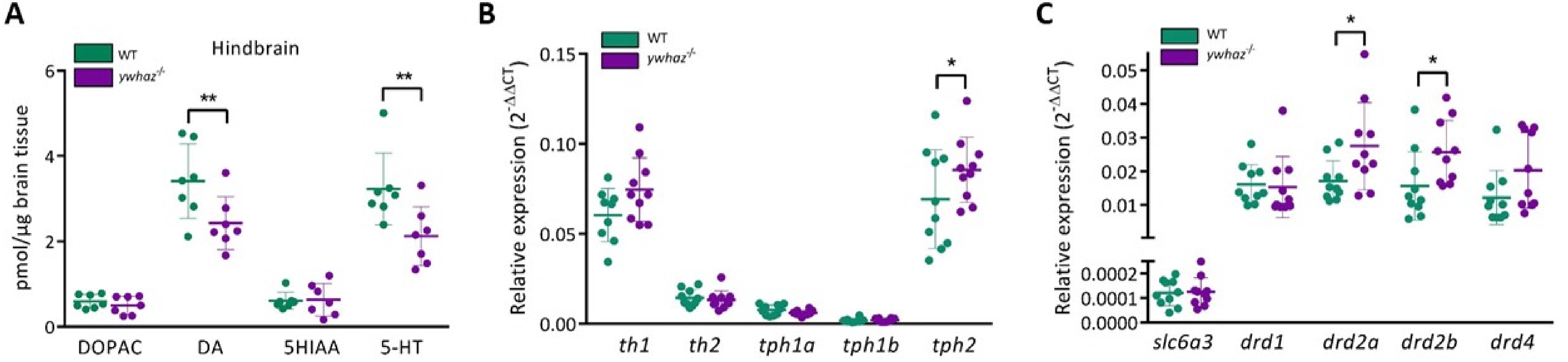

A
WT
ywhaz-/-
Hindbrain
pmol/µg brain tissue
0
2
4
6
**
**
DOPAC
DA
5HIAA
5-HT
B
WT
ywhaz-/-
Relative expression (2-ΔΔCT)
0.00
0.05
0.10
0.15
*
th1
th2
tph1a
tph1b
tph2
C
WT
ywhaz-/-
Relative expression (2-ΔΔCT)
0.0000
0.0001
0.0002
0.01
0.02
0.03
0.04
0.05
*
*
slc6a3
drd1
drd2a
drd2b
drd4

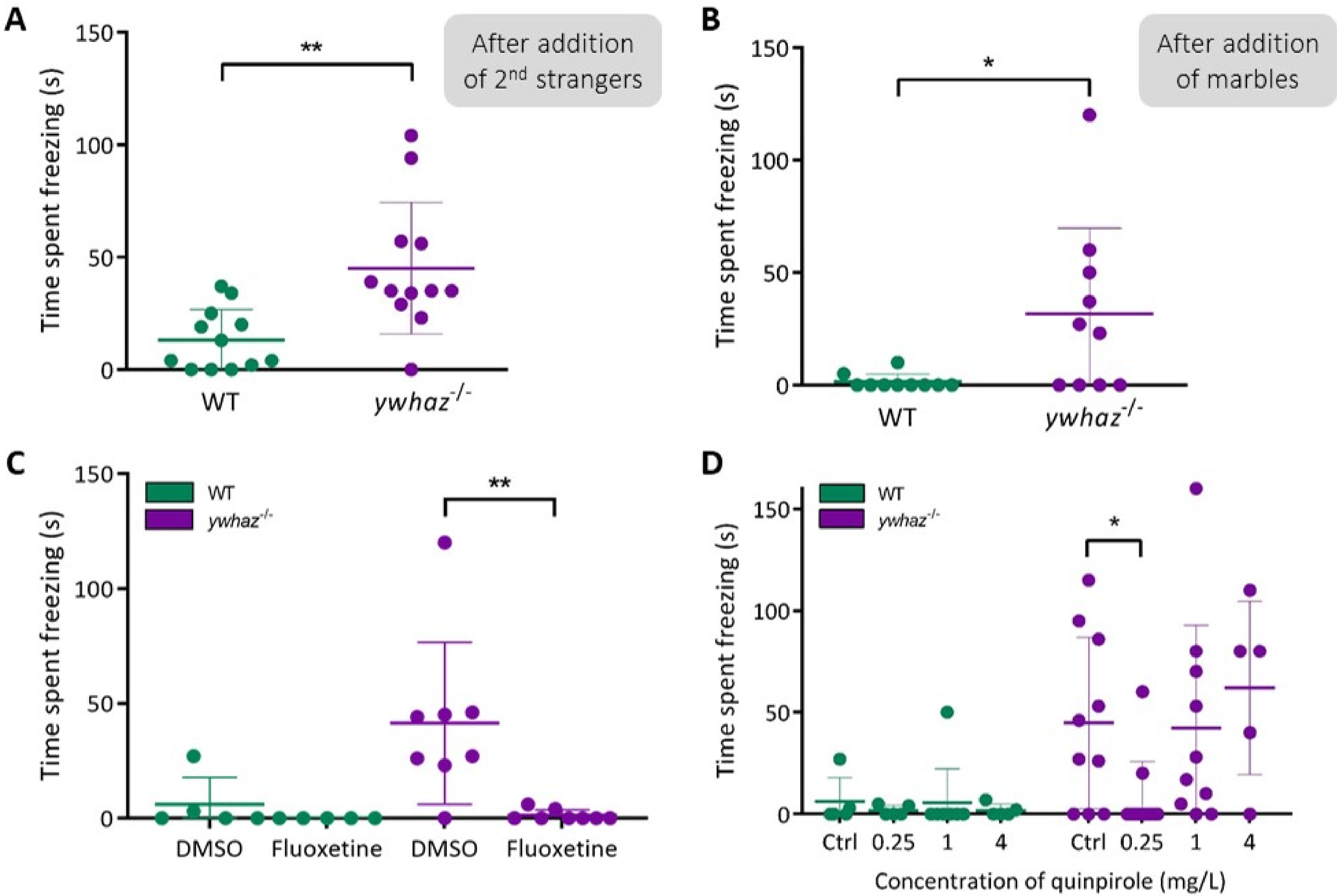

A
After addition of 2nd strangers
**
Time spent freezing (s)
150
100
50
0
WT
ywhaz-/-
B
After addition of marbles
*
Time spent freezing (s)
150
100
50
0
WT
ywhaz-/-
C
WT
ywhaz-/-
**
Time spent freezing (s)
150
100
50
0
DMSO
Fluoxetine
DMSO
Fluoxetine
D
WT
ywhaz-/-
*
Time spent freezing (s)
150
100
50
0
Ctrl
0.25
1
4
Ctrl
0.25
1
4
Concentration of quinpirole (mg/L)